

FR 80 01907

LAPP-TH-02  
12 September 1979



JETS IN LEPTOPRODUCTION FROM QCD

P. Binétruy and G. Girardi

LAPP - Annecy-le-Vieux

ABSTRACT

We review some of the variables used in studying jets in leptoproduction: Stermann-Weinberg distributions, thrust, sphericity, pointing vectors and angular asymmetries.

---

Presented at the "Highly Specialized Seminar: Probing Hadrons with leptons, Erice, 13 - 21 March 1979"

## JETS IN LEPTOPRODUCTION FROM QCD

P. Binétruy and G. Girardi

LAPP, Annecy-le-Vieux, France

## INTRODUCTION

If quarks and gluons are confined, the best way to "see" them is to study the jets of particles. However, while the domain of perturbative QCD has greatly expanded for the last few years, the precision of its predictions has certainly suffered from our lack of methods to handle the non-perturbative features of the theory. In the following, we shall study what perturbative QCD can predict, and also what it cannot. So far, the rule of the game is to find tricks which eliminate non-perturbative effects as much as possible.

Perturbative QCD is a theory of quarks and gluons. One immediately faces two major problems:

- gluons are massless; how do we deal with the infra-red problems?
- physical particles are bound states of quarks and gluons; how do we make the passage from the parton world to hadrons?

The infra-red problem is very similar to the one already extensively studied in electrodynamics. When one computes cross-sections the masslessness of gluons gives rise to divergences of two different kinds. The first one is the infra-red divergence that comes from the emission of soft gluons by a quark. Infinities of this kind are cancelled order by order by the corresponding virtual corrections. For example, the contribution of diagrams shown in Fig. 1a becomes infinite when the mass of the gluon goes to zero but the total contribution of Fig. 1 is finite.

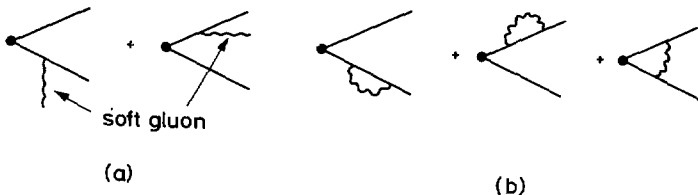


Fig. 1 First order QCD corrections to the emission of two quarks with (a) one real or (b) virtual radiated soft gluon.

The second kind of infinity is the so-called mass or collinear singularity (as shown in Fig. 2). The physical meaning of such a singularity is straightforward: one cannot distinguish between one zero mass particle of momentum  $p$  (i.e., a quark) and two zero mass particles of momenta  $xp$  and  $(1-x)p$ , respectively (i.e., a quark and a gluon). Similarly, the way to get rid of these singularities is obvious: these infinities cancel in the distributions of sufficiently inclusive variables; that is sufficiently inclusive in order not to distinguish between the two preceding processes<sup>1</sup>.

This required feature provides as a bonus an attack on the second problem faced by perturbative QCD: the hadronization of quarks and gluons. For a quantity to be independent of this hadronization process, it must only depend on the properties of a jet as a whole and this condition has been explained in the preceding paragraphs.

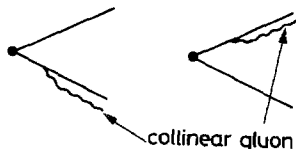


Fig. 2 First order QCD corrections to the emission of two quarks with one gluon radiated collinearly.

We are now in a position to discuss the suitability of different variables. First of all, sphericity is a good example of the limitations of perturbative QCD. It is defined as follows<sup>2</sup>

$$\hat{S} = \frac{3}{2} \min_i \frac{\sum_j |\vec{p}_i^\perp|^2}{\sum_j |\vec{p}_j^\perp|^2} \quad (1)$$

where the sum is over all particles and the  $\vec{p}_i^\perp$  are transverse to a jet axis chosen to minimize  $\hat{S}$ . Two massless quanta of respective momentum  $x p$  and  $(1-x)p$  give a contribution  $[x^2 + (1-x)^2] p_T^2$  to the numerator whereas a single particle of momentum  $p$  gives  $p_T^2$ . The two contributions are obviously different. This means that:

- sphericity is strongly dependent on the hadronization process;
- even when computing cross-sections at the parton level, one encounters, in the course of the calculation, large logarithms of masses that just reflect the fact that sphericity is not an infra-red safe quantity. Sphericity is therefore not computable in perturbative QCD.

A QCD ersatz for sphericity is spherocity<sup>3</sup> whose definition closely follows the preceding:

$$S = \left(\frac{4}{\pi}\right)^2 \min_i \left( \frac{\sum_j |\vec{p}_i^\perp|}{\sum_j |\vec{p}_j^\perp|} \right)^2 \quad (2)$$

Since  $[x + (1-x)]^2 p_T^2 = p_T^2$ ,  $S$  is an infra-red safe quantity (see above).  $S = 0$  for a two-jet event;  $S = 1$  for a spherical event.

Whereas the transverse momentum broadening of the jet is characterized by sphericity, one defines the thrust<sup>4</sup> to study the features of the longitudinal momentum:

$$T = \max_i \frac{\sum_j |\vec{p}_i^\perp|}{\sum_j |\vec{p}_j^\perp|} \quad (3)$$

where  $\Sigma$  runs over all observed particles,  $\tilde{\Sigma}$  over all particles emitted in a hemisphere chosen to maximize  $T$ , and the  $\vec{p}_i^\perp$ 's are transverse to the plane defining the hemisphere (or parallel to its normal, the jet axis).  $T = 1$  for a two-jet event and  $T = \frac{1}{2}$  for a spherical event.

Having recalled the definition of general variables for the study of jets, we will now restrict ourselves to the case of leptonproduction.

### KINEMATICS AND THE SPIRIT OF FIRST ORDER QCD CALCULATIONS

The diagrams contributing in the zeroth and first order to leptonproduction are given in Fig. 3 and 4. In the zeroth order, (Fig. 3) one has just the usual parton model with a two jet structure; the struck parton jet and the proton fragmentation jet. First order QCD corrections give rise to a third jet either coming from a gluon radiated by the quark, (Fig. 4a and b) or from new origin: a gluon in the target proton wave function materializes into a quark-antiquark pair (Fig. 4 c).

We first have to choose the frame in which to study those jets. Whereas the angular correlations that we will discuss in a following section are frame-independent (provided those frames are obtained from one another by a boost along the intermediate vector boson momentum), such a choice is important in thrust and sphericity distributions. The most fashionable frames are:

- a) the lab:  $\vec{p} = \vec{0}$ . Certainly, it is the easiest to obtain experimentally, but unfortunately all distributions are collimated around the vector boson momentum.
- b) The Breit frame:  $\vec{k}_1 + \vec{k}_2 = \vec{0}$ . This frame allows us to get rid of the nucleon remnants since they always go backwards. Streng, Walsh and Zerwas<sup>5</sup> have discussed some nice features of this frame and studied the distribution of a quantity similar to thrust.
- c) The final hadronic state rest frame:  $\vec{p} + \vec{q} = \vec{0}$ . From now on, we shall stick to this frame. It certainly is the frame where the jet structure is the most "open" and where the final state is the most similar to the one encountered in  $e^+e^-$  annihilation, but for the fact that the recoil jet is not simply made of one single parton. The three outgoing partons lie in a plane, which we shall call the hadron plane.

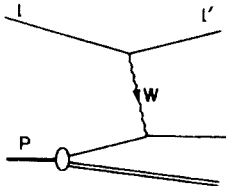
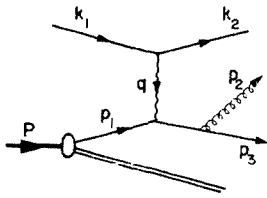
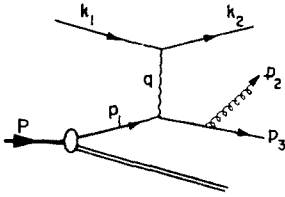
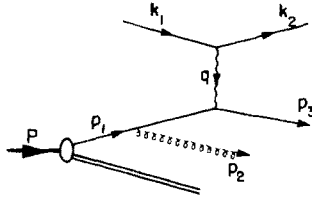


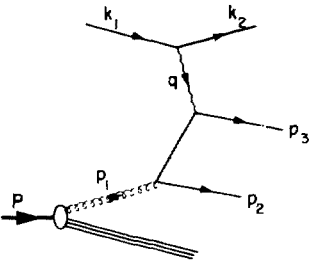
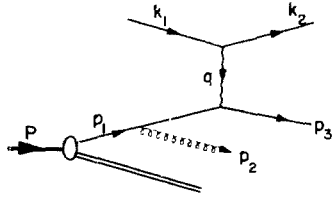
Fig. 3 The zeroth order contribution to two-jet production.



(a)



(b)



(c)

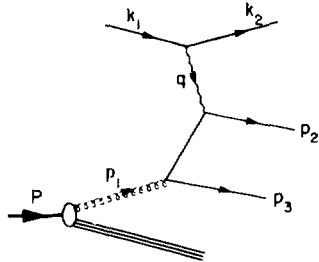


Fig. 4 Contribution of the first order QCD perturbation theory to three-jet events.

- (a) Incident quark;
- (b) Incident antiquark;
- (c) Incident gluon.

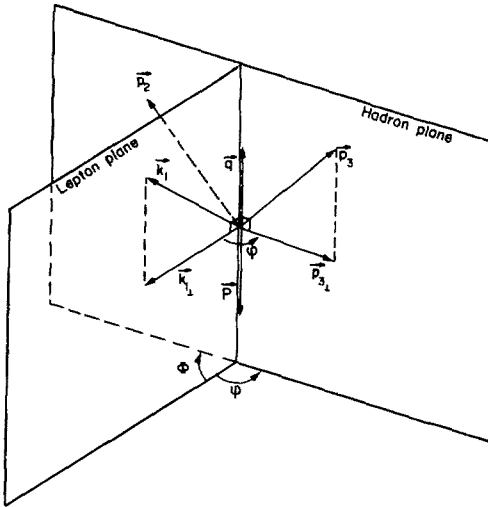


Fig. 5 Kinematic configuration of lepton-hadron scattering in the hadronic final state rest frame.  $\vec{P}, \vec{q}, \vec{p}_1, \vec{p}_2, \vec{p}_3, \vec{k}$  are defined in Fig. 4.

In Fig. 5, we give the kinematic configuration and some definitions. We also define the total hadronic energy  $W^2 = (P + q)^2$ ;  $y = (\vec{p}_1 \cdot \vec{q}) / (p_1 \cdot k_1)$ ; and  $x_i = 2E_i/W$  where  $E_i$  is the energy of the  $i^{\text{th}}$  outgoing quantum.

We now come to thrust and sphericity. The definitions given above were originally proposed for the  $e^+e^-$  annihilation case. The main difference between this case and leptonproduction is that we now have an axis defined by  $\vec{q}$ . One could then try to define new variables, taking this fact into account<sup>6</sup>. Unfortunately, it seems that experimental uncertainties in the determination of  $\vec{q}$  undermine the usefulness of such variables. So we keep the original definitions of thrust and sphericity.

These quantities have been computed by De Rújula et al.,<sup>7</sup> for a three-quantum final state. Their results still hold:

$$T = 2 \max \frac{\sum_{i=1}^3 |\vec{p}_i''|}{\sum_{i=1}^3 |\vec{p}_i|} = \max (x_1, x_2, x_3) \geq \frac{2}{3} \quad (4)$$

$$S = \left(\frac{4}{\pi}\right)^2 \min \left( \frac{\sum_{i=1}^3 |\vec{p}_i^i|}{\sum_{i=1}^3 |\vec{p}_i^i|} \right)^2 = \frac{64}{\pi^2} (1-x_1)(1-x_2)(1-x_3)/T^2 \quad (5)$$

### STERMAN-WEINBERG JET FORMULA

Mainly for illustrative purposes, we begin by describing the Sterman-Weinberg approach as applied to leptonproduction. Sterman and Weinberg<sup>8</sup> define and compute the fraction of two-jet events  $f(\epsilon, \delta)$  for  $e^+e^-$  annihilation in which a fraction of the total hadronic energy smaller than  $\epsilon$  is emitted outside two opposite cones of aperture angle  $2\delta$ . We shall keep this definition for leptonproduction (for another point of view, see Ref. 6). This quantity is obviously infra-red finite. Requiring that a fraction  $\epsilon$  of the energy  $W$  is emitted outside the cone eliminates the emission of soft gluons that one cannot handle and giving a finite aperture  $2\delta$  to the cone integrates the collinear singularities already discussed. Of course, when one puts  $\epsilon$  or  $\delta = 0$ , the infra-red divergences creep in again. This is easily seen<sup>9</sup> in Fig. 6 which shows  $1 - f(\epsilon, \delta)$  as a function of  $\delta$ , at fixed  $\epsilon$ . For small enough  $\epsilon$  or  $\delta$ ,  $1 - f$  becomes large and the calculation in first order in  $x_s$  is no longer reliable.

If we want the results of Fig. 6 to be meaningful, we have to compare them with a two jet model with a finite transverse momentum spread. We choose the simplest parametrization of  $f(\epsilon, \delta)$  for such a model, namely, at fixed  $\epsilon$ :

$$f_{NP}(\epsilon, \delta) = 1 - e^{-\delta^2/(\Delta\delta)^2} \text{ with } \Delta\delta = n(W) \frac{\langle p_T \rangle}{\epsilon W} \quad (6)$$

For numerical results, we take  $\langle p_T \rangle$  to be 300 MeV and<sup>10</sup>

$$n(W) = \frac{3}{2} \left( \frac{2}{3} + 1.28 \ln W^2 \right)$$



The motivations for Eq. (6) are the following: since  $\delta$  is strongly related to the transverse momentum, we take a gaussian, remembering the behaviour in  $e^{-4P_T^2}$  observed experimentally. Moreover, when  $\delta \rightarrow 0$  or  $\epsilon \rightarrow 0$ ,  $f(\epsilon, \delta) \rightarrow 0$ , as one could naively expect. The dashed curves of Fig. 6 show the behaviour of  $f_{NP}(\epsilon, \delta)$ . One can see at once that, at presently available energies, the perturbative QCD result is completely lost in the non-perturbative background. The hope is that, at higher energies, as  $\Delta\delta \propto 1/W$  decreases and  $f_{NP}(\epsilon, \delta)$  shrinks around  $\epsilon = 0$ , the perturbative curves will show up.

We will refine these gross results in the following section but the conclusions will not change dramatically.

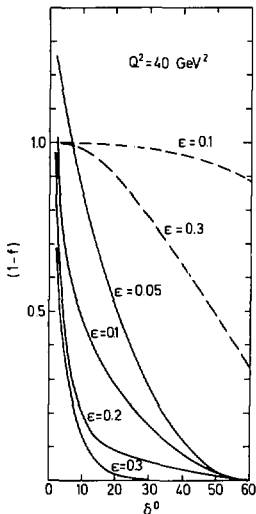


Fig. 6  $1 - f$  as a function of  $\delta$  at fixed  $\epsilon$  and  $Q^2$ .

After calculating diagrams of Fig. 4 and then changing to the suitable variables, it is straightforward to get<sup>10,11</sup>

$$\left| \frac{1}{\sigma} \frac{d\sigma}{dT} \right| (Q^2, W^2) = \left| \frac{d\sigma^{(o)}}{dQ^2 dW^2} \right|^{-1} \frac{d\sigma}{dQ^2 dW^2}$$

where  $\sigma^{(o)}$  is the two-jet cross-section.

The first question of importance is to study  $Q^2$  and  $W^2$  dependence. There are two arguments which tend to opposite conclusions.

First,  $(1/\sigma)(d\sigma/dT)$  is of order  $\alpha_s(Q^2)$  where  $\alpha_s(Q^2)$  is the running coupling constant

$$\alpha_s(Q^2) = \frac{4\pi}{9} \frac{1}{\ln(Q^2/\Lambda^2)}, \quad \Lambda = 500 \text{ MeV} \quad (7)$$

chosen to depend on  $Q^2$  (and not  $W^2$ ) because  $Q^2$  is the only relevant variable for parton diagrams of the type given in Fig. 4. Second,  $W$  is the natural variable for the hadronic final state, in particular for the three jet distribution. Figure 7 shows the actual  $Q^2$  dependence for the QCD distribution. It suggests that the  $Q^2$  dependence in  $\alpha_s$  is damped and that  $W$  is the natural variable.

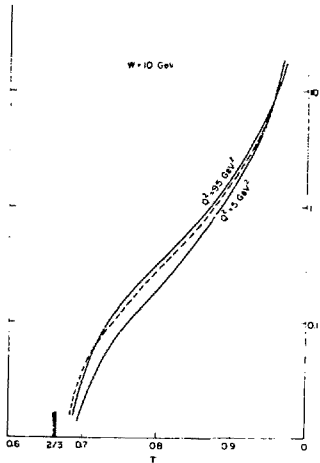


Fig. 7  $Q^2$  dependence of  $(1/\sigma) d\sigma/dT$  at  $W^2 = 100 \text{ GeV}^2$ . The dashed curves is the  $Q^2$  integrated version of this distribution.

The reason for this fortunate behaviour is, of course, kinematic. Let us write the relation between the fraction of momentum  $\xi$  carried by the struck parton and the fraction  $x$  of energy carried by the nucleon remnant jet

$$1 - \xi = \frac{W^2}{W^2 + Q^2} x_1 \quad (8)$$

If the gluon is collinear to the emitted quark, one has  $x_1 = T$  and

$$T = (1 - \xi) \left(1 + \frac{Q^2}{W^2}\right) = \frac{1 - \xi}{1 - x} \quad (9)$$

where  $x = Q^2/2Mv$  is Bjorken  $x$ . This gives a thrust distribution determined by the  $\xi$  distribution and, if one neglects dynamics, a thrust distribution approximately  $Q^2$  independent and peaking at

$$T_{\max} = \frac{2}{3} \left(1 + \frac{Q^2}{W^2}\right) = \frac{2}{3} \frac{1}{1-x} \quad (10)$$

Of course, nothing like this can be seen in Fig. 7 because of the infra-red divergence at  $T = 1$ . Actually, the expression that one gets for  $(1/\sigma)(d\sigma/dT)$  includes terms in  $\alpha_s(Q^2) \ln(1 - T)/(1 - T) \sim 1$  that are of the order  $[\alpha_s(Q^2)]^0$  and give a contribution to the two-jet distribution. But one can imagine that if one could handle the infra-red divergence, such behaviour would show up.

Now, as  $Q^2$  increases,  $T_{\max}$  approaches 1 and the tail of the distribution becomes broader. At the same time this tail is of order  $\alpha_s(Q^2)$  which tends to decrease. The two effects compensate.

We can now integrate over  $Q$  and obtain  $[(1/\sigma)/(d\sigma/dT)](W^2)$ . Of course, such a result is of little practical interest since it deals with quarks and gluons, and we have to "treat" it in order to compare it with experiments.

The way to do it has been suggested by De Rújula et al.,<sup>7</sup> and from now on we closely follow their procedure. It consists in smearing the above results over bins of thrust of width  $\Delta T_{np}$  to take into account the hadronization of quarks and gluons.  $\Delta T_{np}$  is taken to be

$$\Delta T_{np} = \frac{1}{2} n(W) \frac{\langle p_{\perp} \rangle}{W} \quad (11)$$

where  $n(W)$  and  $\langle p_T \rangle$  have been defined in formula (6). On the same basis, the zeroth order (two jets) distribution  $\delta(1-T)$  at the parton level gets broadened by the non-perturbative effects. We choose a simple parametrization similar to (6)

$$\frac{1}{\sigma_0} \left( \frac{d\sigma}{dT} \right)_{NP} = \frac{2}{(\Delta T_{NP})^2} (1-T) e^{- (1-T)^2 / (\Delta T_{NP})^2} \quad (12)$$

Here the factor  $(1-T)$  accounts for the fact that two massive particles cannot be collinear [one can also easily check that Eq. (12) is compatible with Eq. (6)].

Results are shown in Figs 8 and 9. At presently available energies (Fig. 8) the situation seems hopeless. But for higher  $W$ 's (Fig. 9), the QCD tail starts emerging from the non-perturbative background.

It is certainly quite instructive to compare our results with those in  $e^+e^-$  annihilation<sup>7</sup>: the QCD tail is smaller in leptoproduction than in  $e^+e^-$  by roughly a factor of two. On the other hand, one can easily check from the formulas of Ref. 10, that the leading term in thrust distribution (i.e.,  $\ln(1-T)/(1-T)$ ) is the same for the two processes. This looks encouraging because it implies a kind of universality between the two processes, which is not surprising when one compares the QCD diagrams) and now experimentalists are starting to find such similarities<sup>12</sup>. We are tempted to explain the apparent discrepancy between the two results by the same kinematic argument as before: quark distributions favour thrust around  $T_{max} \sim 1$  and therefore disfavour the QCD tail.

From the thrust distribution, we can infer mean values for thrust and sphericity. We give  $\langle S \rangle$  in Fig. 10 and compare it with a two-jet non-perturbative value that we choose to be:

$$\langle S \rangle_{NP} = \left( \frac{4}{n} \right)^2 \frac{\langle P_1 \rangle^2}{W^2} \langle n(W) \rangle^2 \quad (13)$$

where all quantities have already been defined. The left side of the figure gives the situation for  $\nu p$  scattering at variable energies. As one could expect, the perturbative three-jet results are completely lost in the two-jet background. The right part gives  $\langle S \rangle$  for ep scattering at  $E_{lab} = 20\ 000$  GeV (as one could find in a next generation ep colliding machine). Of course, the situation improves and the QCD tail shows up.

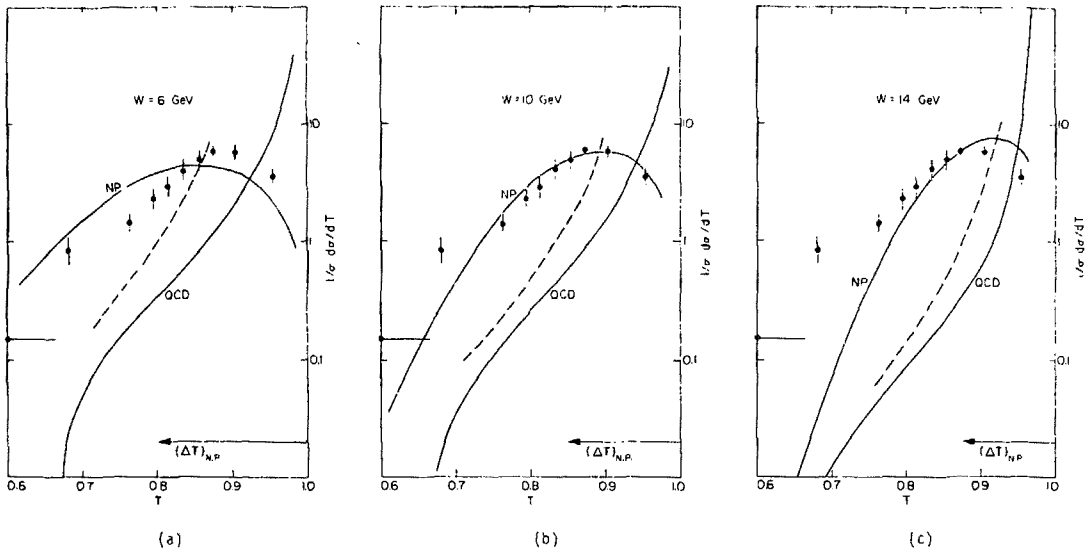


Fig.8  $(1/\sigma)(d\sigma/dT)$  for various values of  $W$ , integrated over  $Q^2 > 1 \text{ GeV}^2$ ,  $E_{\text{lab}} = 100 \text{ GeV}$ . Data from Ref. 13 correspond to a distribution integrated over  $6 < W < 10 \text{ GeV}$  and should therefore be applied only to  $W = 10 \text{ GeV}$ . N.P. stands for the non-perturbative distribution given in Eq. (12). The dashed curves correspond to the QCD contribution smeared over bins of with  $\Delta T_{\text{NP}}$  indicated in the figures.

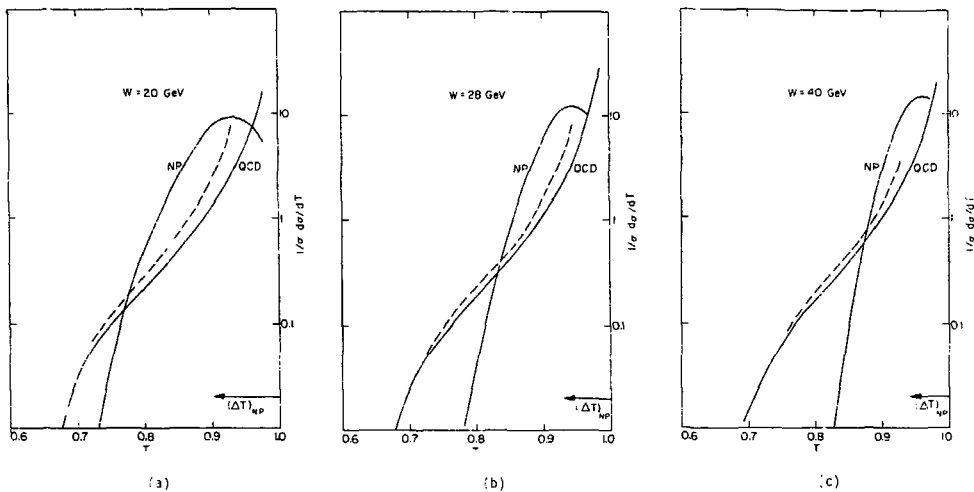


Fig. 9 Analogous to Fig. 8 for larger values of  $W$ .

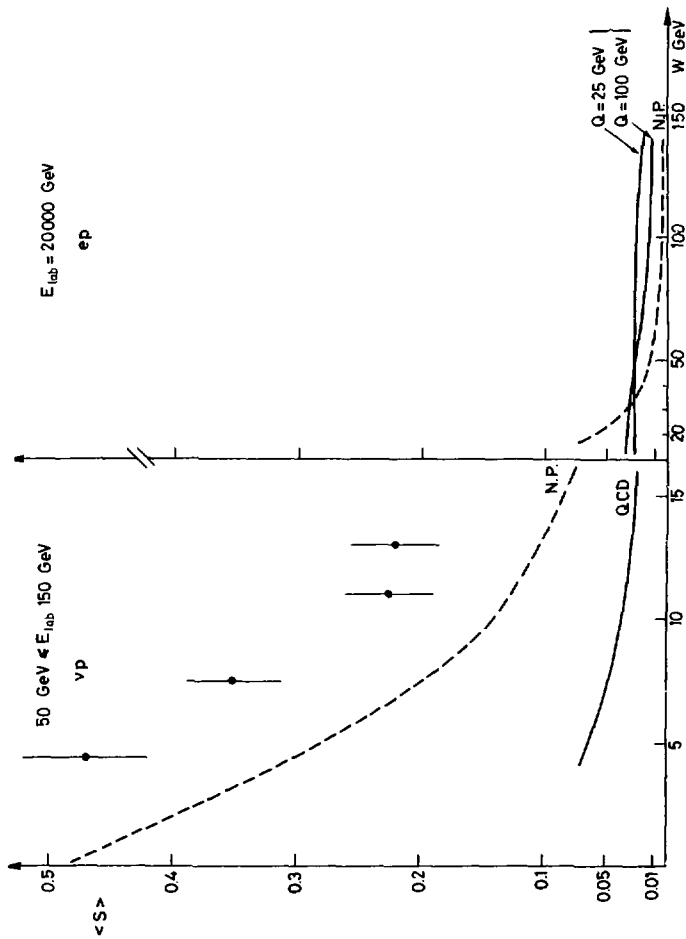


Fig. 10.  $\langle S \rangle$  as a function of  $W$  for  $\nu p$  scattering ( $W < 15$  GeV,  $50 \text{ GeV} < E_{\text{lab}} < 150 \text{ GeV}$ ) at  $e p$  scattering ( $15 \text{ GeV} < W < 150 \text{ GeV}$ ;  $E_{\text{lab}} = 20\,000 \text{ GeV}$ ). The N.P. dashed lines give the values of  $\langle S \rangle_{\text{N.P.}}$ , the solid lines give the QCD perturbative result, (and experimental points are from Ref. 13. Buras-Gaemers parametrization for structure functions has been used<sup>14</sup>).

We end this section by discussing the pointing vector. Roughly speaking, the pointing vector measures the energy flow in the hadron plane as a function of angle. More precisely, it is defined as<sup>7</sup>

$$P(Q, W, T, \theta) = \frac{1}{\sigma(\theta)} |P| \frac{d\sigma}{dT d\cos^2\theta} \quad (14)$$

For a careful definition of this quantity, see M.K. Gaillard's talk; for the experimental difficulties in measuring it, see H. Meyer's contribution to these proceedings.

(o) The only difference with the  $e^+e^-$  case is that we divide by  $\sigma(\theta)$  in order to eliminate the Q and W dependence of the zeroth order.

It is, of course, of no use to give our estimate of the pointing vector at present energies where the background is so important. So, Fig. 11 gives the predictions for energies available in a high-energy ep colliding machine.

#### ANGULAR ASYMMETRIES

The distribution in the azimuthal angle  $\phi$ , defined earlier, introduces angular asymmetries whose importance was first stressed by Georgi and Politzer<sup>15</sup>. Cahn<sup>16</sup> has clarified their origin: the initial transverse momentum of the struck quark. Let us sketch his procedure.

First, if  $y = 1$ , [that is if the incident lepton (neutrino) is collinear with  $\vec{q}$ ], there is no preferred direction in the plane transverse to  $\vec{q}$  and therefore no asymmetry. On the other hand, if  $y \neq 1$ , there is a preferred direction along  $\vec{k}_1$  (see Fig. 5). One can easily show, for example, on dimensional grounds, that the squared amplitude is of order  $S$ , where  $S$  is the energy available in the center-of-mass of the incident particles (quark neutrino). If we fix all momentum components parallel to  $\vec{q}$ , the situation where the struck quark is antiparallel to the neutrino in the transverse plane is favoured, since it maximizes  $S$ . Since  $q_T = 0$ , the emitted quark has the same transverse momentum as the struck quark.



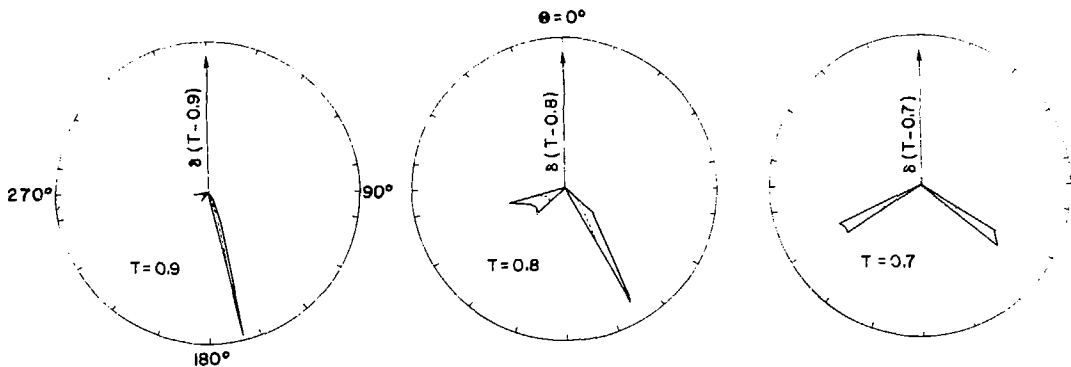


Fig. 11. Pointing vector for different values of thrust at  $E_{\text{cm}} = 20\,000 \text{ GeV}$ .  
 Solid lines:  $Q^2 = W^2 = 1\,280 \text{ GeV}$ ; dashed lines  $Q^2 = W^2 = 8\,000 \text{ GeV}^2$ .  
 Different scales have been used for the different values of thrust.

The origin of this initial transverse momentum is twofold: either it is the radiation of a gluon by the quark, before its interaction with the current, or a primordial  $p_T$  of the quark in the nucleon.

The asymmetries between the lepton plane and an outgoing hadron have been extensively studied<sup>15-20</sup> (see also P. Landshoff's talk in these Proceedings). They have three disadvantages: first, one loses most of the information by representing the final state by a single hadron; second, one has to use poorly known fragmentation functions; and third, it is hard, at present energies to disentangle the two origins of transverse momentum.

The asymmetries between the lepton plane and an outgoing jet would be worth studying if one could distinguish between a quark and a gluon jet. Let us only note that, since the quark is preferentially emitted opposite to the incident lepton, the gluon is preferentially radiated on the same side (see Fig. 5).

Finally, we define the angle  $\phi$  between the lepton plane and the hadron plane and study corresponding asymmetries<sup>10</sup>. Whereas the definition of a parton plane is obvious (see Fig. 5), we define the hadron plane by minimizing the momentum of all hadrons out of this plane. Since  $\phi$  is an angle between planes, we restrict it to the range  $-\pi/2 \leq \phi \leq +\pi/2$ . It is straightforward to see that  $\phi$  suffers infra-red divergences: when the gluon becomes collinear to a quark, it is no longer possible to define a plane. We therefore, have to make cuts in thrust in order to prevent such a situation.  $\phi$  is then an infra-red safe quantity since a quark or a quark plus an extra collinear gluon will give the same contribution.

Results are shown in Figs 12-14 for various cuts in thrust ( $T < 1 - \Delta T$ ). One can see that the effects are sizeable even for large cuts in T.

If we make the following assumption on non-perturbative effects (hadronic broadening of jets are rotationally invariant with respect to the jet axis) then those effects are expected to occur at a much lower level than in the previous cases. Two jet events will be cylindrical and will therefore give "no contribution" to the statistical determination of a plane. Moreover, a primordial transverse momentum will shift only slightly the thrust distribution and, thanks to the cuts in T, give no important contribution to the  $\phi$  asymmetry.

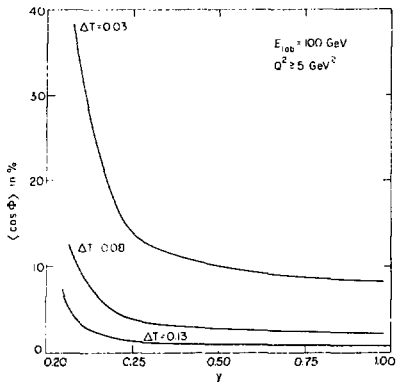


Fig. 12 Angular asymmetry between the hadron and lepton planes  $\langle \cos \Phi \rangle$  integrated over  $Q^2, S, T$  ( $2/3 < T < 1 - \Delta T$ ) as a function of  $y$ .

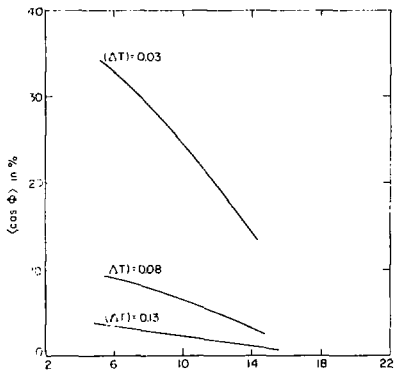


Fig. 13 Same as Fig. 12,  $\langle \cos \Phi \rangle$  as a function of  $W$ .

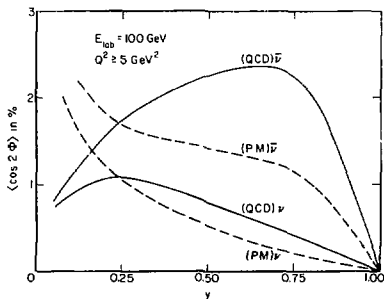


Fig. 14.  $\langle \cos 2\Phi \rangle$  as a function of  $y$ .

## CONCLUSION

Leptonproduction processes are much richer processes than  $e^+e^-$  annihilation since they involve more variables ( $W, \phi$ ), a new axis ( $\vec{q}$ ) and a choice between different reference frames. Unfortunately, the situation is not as clearcut as in  $e^+e^-$  because we have to deal with uncertainties in the structure functions, experimental difficulties in determining the  $q$  vector (at least, in neutrino processes), and our ignorance of the behaviour of nucleon remnants. It is therefore difficult to find clean tests for QCD from jet studies. We believe that the study of the  $\Phi$  asymmetries may be an exception.

## ACKNOWLEDGEMENTS

One of us (P.B.) thanks J.J. Aubert and G. Preparata for giving him the opportunity to participate in the Erice workshop.

REFERENCES

1. T. Kinoshita, J. Math Phys. 3: 650 (1962);  
T.D. Lee and M. Nauenberg, Phys. Rev. 133:B 1549 (1964).
2. J.D. Bjorken and S.J. Brodsky, Phys. Rev. D1: 1416 (1970).
3. H. Georgi and M. Machacek, Phys. Rev. Letters 39: 1237 (1977).
4. E. Farhi, Phys. Rev. Letters 39: 1587 (1977).
5. K.H. Streng, T.F. Walsh and P.M. Zerwas, DESY 79/10 (February 1979).
6. P.M. Stevenson, Nucl. Phys. B150: 357 (1979) and preprint  
ICTP/78-79/16 (April 1979).
7. A. de Rújula, J. Ellis, E.G. Floratos and M.K. Gaillard,  
Nucl. Phys. B138: 387 (1978).
8. G. Sterman and S. Weinberg, Phys. Rev. Letters 39: 1436 (1977).
9. P. Binétruy and G. Girardi, Phys. Letters 83B: 382 (1979).
10. P. Binétruy and G. Girardi, Nucl. Phys. B155:150 (1979).
11. Ranft and Ranft, Leipzig University preprint 78-15 (1978).
12. Aachen-Bonn-CERN-London I.C.-Oxford-Saclay Collaboration  
CERN/EP 79-39 Rev. (1979);  
M. Derrick et al., Preprint ANL-HEP-PR-79-17 (1979).
13. A. Vayaki et al., Aachen-Bonn-CERN-London-Oxford-Saclay  
Collaboration, CERN/EP/PHYS 78-28 (1978). Note that in  
Fig. 5c of this paper, the correct scale is  $(1/\sigma)(d\sigma/dT) \times 10$   
and not  $(1/\sigma)(d\sigma/dT) \times 10^2$ .
14. A.J. Buras and K.J. F. Gaemers, Nucl. Phys. B132: 249 (1978).
15. H. Georgi and H. D. Politzer, Phys. Rev. Letters 40: 3 (1978).
16. R.N. Cahn, Phys. Lett. 78B: 269 (1978).
17. A. Méndez, Nucl. Phys. B145: 199 (1978);  
A. Méndez, A. Raychaudhuri and V.J. Stenger, Nucl. Phys.  
B148: 499 (1979).
18. J. Cleymans, Phys. Rev. D18: 954 (1978).
19. G. Köpp, R. Maciejko and P.M. Zerwas, Nucl. Phys. B144: 123  
(1978).
20. P. Mazzanti, R. Odorico and V. Roberto, Preprint IFUB/78-11.

